Bull. Chem. Soc. Jpn., 71, 2597—2601 (1998)

Crystal Growth of Perylene Microcrystals in the Reprecipitation Method

Hitoshi Kasai, Hidetoshi Oikawa, Shuji Okada, and Hachiro Nakanishi*

Institute for Chemical Reaction Science, Tohoku University, 2-1-1 Katahira, Aoba-ku, Sendai 980-8577

(Received June 3, 1998)

The crystal growth of α-perylene microcrystals in the reprecipitation method was studied using of light-scattering technique and absorption spectroscopy. A certain model for microcrystallization has been established. The relationship between the reprecipitation conditions and the crystal size was clarified on the basis of this model. Especially, the water temperature was confirmed to be one of the most important parameters used to control the size of the microcrystals in the reprecipitation method. The apparent activation energy for the microcrystallization of perylene was estimated to be 68 $\mathrm{kJ\,mol^{-1}}$.

There are many fascinating phenomena in nanometer-order microcrystals.[1—8] Some scientists have theoretically predicted that an electron-hole interaction in a semiconductor microcrystal would be different from that in the same bulk crystal, owing to a quantum-confinement effect.[3—6] In fact, the nonlinear optical (NLO) properties of semiconductors were reported to be enhanced through microcrystallization.[7,8] In organics, multiple quantum wells produced by means of a molecular-beam deposition technique exhibited a one-dimensional confinement effect, which affected such optical properties as the absorption and emission.[9—11] Organic microcrystals, however, have so far been paid little attention, because of fabrication difficulties.[12,13]

We have succeeded in preparing some organic microcrystals by the reprecipitation method,[14] and have found some interesting optical properties.[15—21] For example, even though the crystal size of prepared perylene microcrystals was greater than 100 nm, the absorption and emission spectra were observed to be clearly dependent on the crystal size.[15—18] Microcrystal dispersion liquids hardly scatter light, because the crystal size is usually smaller than the incident-light wavelength. In addition, microcrystals were stably dispersed for more than half a year. Therefore, some polydiacetylene microcrystal dispersion liquids with a low optical-loss and a large $\chi^{(3)}$ system were expected to be promising optical Kerr shutter materials, even in the case of a concentrated dispersion.[20,21]

We also tried to clarify the crystal-growth mechanism of microcrystals in the reprecipitation process in order to prepare smaller microcrystals.[22,23] As a result, in most of the compounds, like diacetylene and dyes, microcrystallization was found to be completed just after reprecipitation. In the present study, we investigated the crystal-growth process of perylene microcrystals by measuring the light scattering and absorption spectroscopy; another mechanism involving microcrystallization in the reprecipitation method will also be discussed.

Experimental

Preparation of Perylene Microcrystals. The perylene used was purified by vacuum sublimation, and succeeding zone refining. The typical condition for preparing perylene microcrystals by the reprecipitation method was as follows:[14] 0.1 ml of a perylene acetone solution (ca. 10^{-3} M) (1 M = 1 $\mathrm{mol\,dm^{-3}}$) was quickly injected using a microsyringe into 10 ml of distilled water stirred vigorously at room temperature. As a result, perylene microcrystals were found as a pale-yellow water dispersion.

Spectroscopy and Scanning Electron Microscope. The UV-visible absorption spectra of perylene microcrystals dispersed in water were measured using a Shimadzu UV-240. The size and shape of the microcrystals were observed by means of a Hitachi S-900 scanning electron microscope (SEM). The size and its distribution of microcrystals dispersed in water were also evaluated by the dynamic light-scattering (DLS) technique using Otsuka Electronics DLS-7000. The static scattered light intensity (SLS) from the microcrystal dispersion was also monitored by the same instrument.

Results

Absorption Spectra of Perylene Microcrystals in the Preparation Process. Figure 1 shows the change in the absorption spectra of perylene microcrystals with the elapsed time after injection of the solution at room temperature. The excitonic absorption-peak positions were shifted from 451 to 460 nm within three hours, and the peak half-width became broad within the same period. As already reported elsewhere,[15] the excitonic absorption peak positions in the steady-state were around 450 and 470 nm for 50 and 200 nm in crystal size, respectively. The absorption spectrum of α-perylene bulk crystals had been measured through the (001) plane a long time ago.[24] There, in the case of using light polarized parallel to the b-axis, the excitonic absorption peak position was reported to be 21400 $\mathrm{cm^{-1}}$ (467 nm). Thus, the spectral changes shown in Fig. 1 are considered to reflect the crystal growth of microcrystals. The absorption peak shifted to a longer wavelength and their broadening occurred more rapidly at higher temperature.

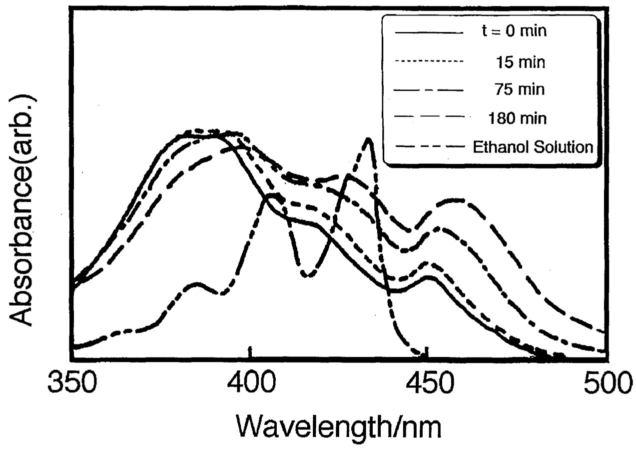

Fig. 1. Change of absorption spectra of perylene microcrystals after injection at room temperature in the reprecipitation method.

SEM Observation of Perylene Microcrystals with Different Sizes. Figure 2 shows SEM micrographs of perylene microcrystals which were collected on a Millipore filter after filtration. Two kinds of samples were prepared under different reprecipitation conditions: Sample (a) was obtained by heating for three hours at 70 °C, and cooling down to r.t.; sample (b) was obtained by keeping for 16 h at 7 °C, and keeping back to r.t. The crystal sizes of both samples (a) and (b) were determined to be about 200 nm and about 120 nm from SEM observations, respectively. These values agreed roughly with those determined by DLS.

Morphology of Perylene Microcrystals Prepared. The crystal structure of perylene microcrystals was clarified to be of the α-type by measurements with X-ray power diffraction, the pattern of which was almost similar to that of bulk crystals.

SLS Measurements of Water Dispersion of Perylene Microcrystals in the Preparation Process. The intensity of SLS (I_S) was monitored during the microcrystallization process in the reprecipitation method. Figure 3 indicates the changes of I_S/I_0 with various injected amounts of 10^{-2} M solution into 10 ml of water at 70 °C. I_0 is the incident laser-beam intensity. Though I_S/I_0 was very small just after injection, it increased, and then became saturated, during the course of microcrystalization. The final I_S/I_0 values were approximately proportional to the amount of injected solution.

Figure 4 shows the dependence of I_S/I_0 on the water temperature. The crystal growth rate became rapid upon elevating the temperature. Interestingly, the final I_S/I_0 values became almost the same at above 35 °C, and the microcrystal sizes attained were the same within the experimental error. On the other hand, the final I_S/I_0 values below 35 °C were different from those above 35 °C. In fact, smaller microcrystals were found below 35 °C.

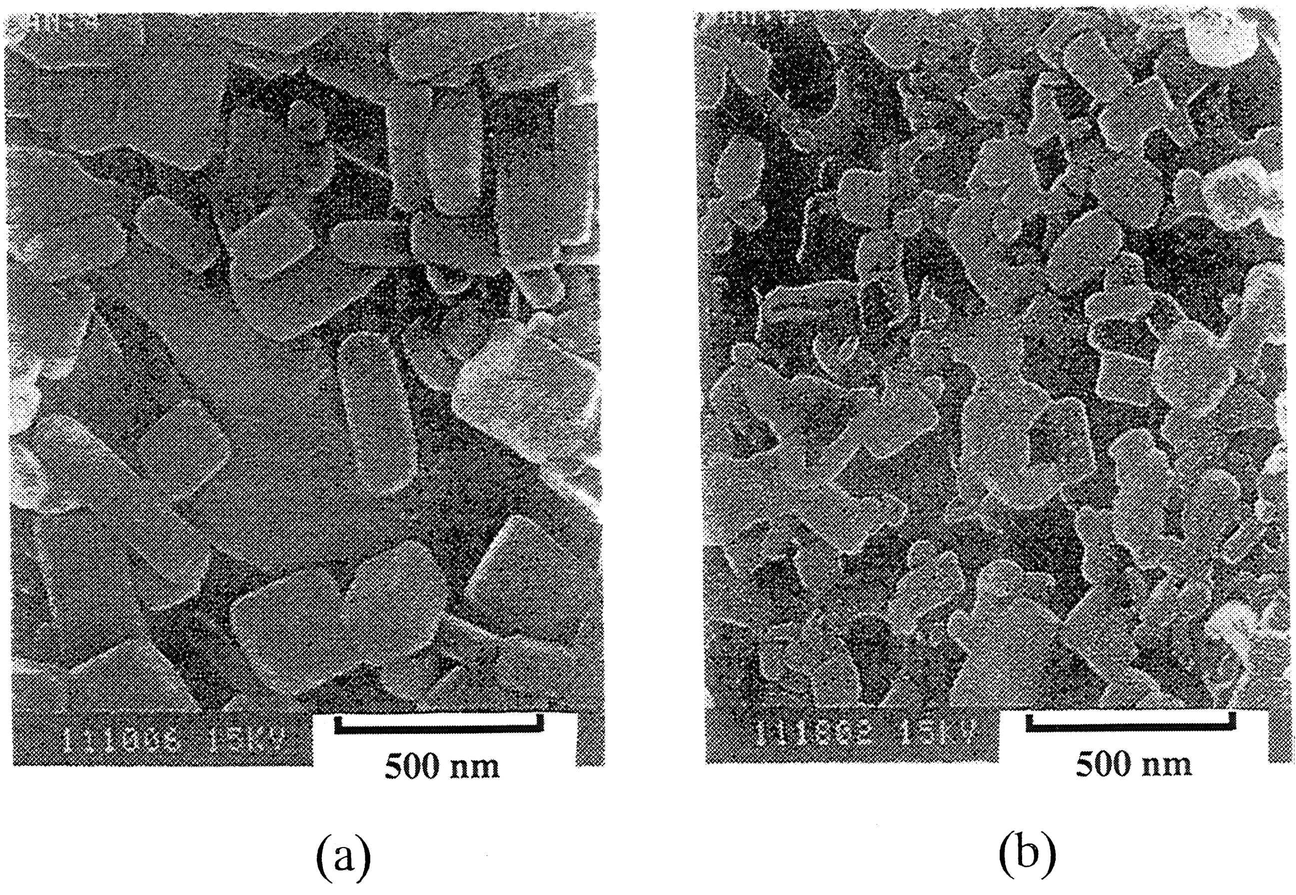

Fig. 2. SEM micrographs of perylene microcrystals collected on a Millipore filter. Each sample was obtained (a) 70 °C for three hours; (b) at 7 °C for 16 h.

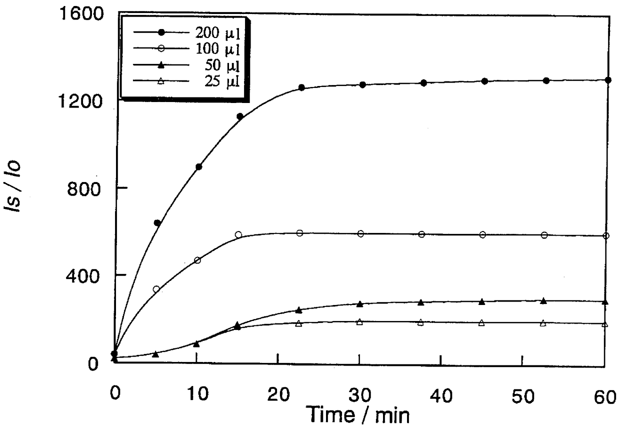

Fig. 3. Change in I_s/I_o after injecting various amounts (●: 200 μl, ○: 100 μl, ▲: 50 μl, △: 25 μl) of 10^{-2} M solution into 10 ml of water at 70 °C.

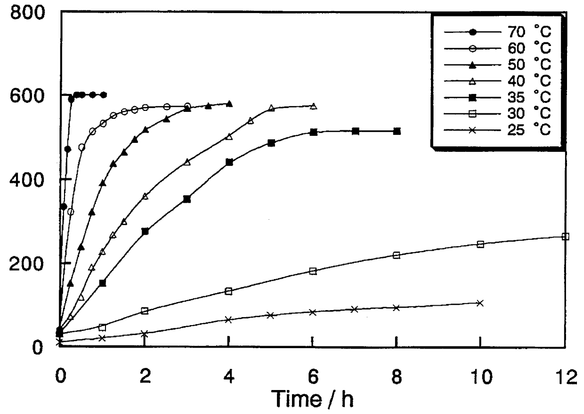

Fig. 4. Dependence of I_s/I_o on water temperature after injecting various amounts of 10^{-2} M solution into 10 ml of water.

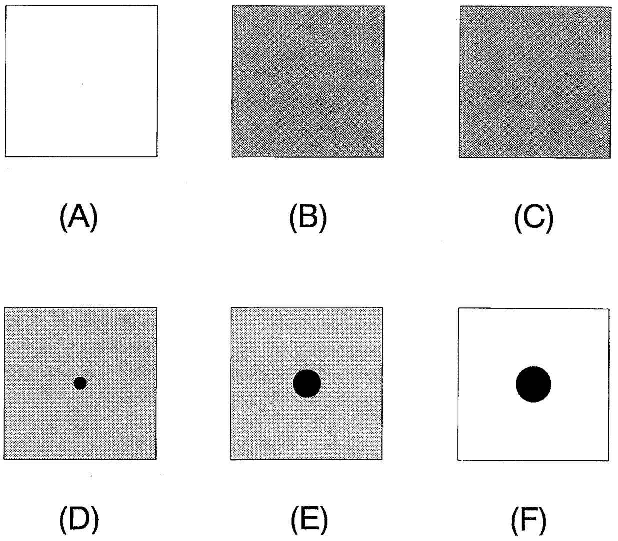

Fig. 5. Model of simplified microcrystallization process of perylene in the reprecipitation method.

Discussion

Investigation of Crystal Growth Process of Perylene Microcrystals Using an Model. Let us consider the process of microcrystallization according to the model shown in Fig. 5. Each figure shows a certain portion of water dispersion. Figure 5(A) displays water before the injection of a perylene solution, and no light is scattered. Just after the injection of a solution, ultrafine droplets of perylene solution are first found, and the solvent in the first droplets is dissolved in water to give perylene clusters with a constant number, determined by the experimental conditions, as shown in Fig. 5(B). The contrast in the background of Fig. 5 indicates the number density of perylene clusters, and the darker background shows a higher density of the clusters. The fact that perylene is not molecularly dispersed in water at this stage is confirmed by the absorption spectrum, which is completely different from that in solution. Then, nuclei for microcrystallization are generated in Fig. 5(C), where the dot at the center is a crystal nucleus. All of the nucleation is assumed to be generated in a complex way at this stage. In other words, the number of nuclei is said to be in equilibrium with the number of microcrystals. Thus, in the volume shown in Fig. 5, only one nucleus appears for simplicity. Crystal growth proceeded by aggregating clusters to a nuclei, resulting in a larger size of the crystal (drawn by a black circle and lower density of clusters, as shown in Fig. 5(D) to Fig. 5(E)). Figure 5(F) is the final stage, in which almost all clusters in this volume of dispersion are included in a microcrystal.

For a semi-quantitative discussion using the above model, the light scattering of this dispersion system is considered to be only according to a theory of Rayleigh. The scattered light intensity (I_s/I_o) is expressed by

$$\frac{I}{I_o} = \frac{2\pi^2 V^2 N}{r^2 \lambda^4}\left(\frac{\varepsilon - \varepsilon_0}{\varepsilon_0}\right)^2 \left(1 + \cos^2\theta\right), \tag{1}$$

where V and N are the volume and number of scattering bodies, respectively; r is the distance between the scattering body and the detector, λ is the wavelength of the incident laser, ε and ε_0 are the dielectric constants of the scattering body and the medium, and θ is the scattering angle. In the above model, the crystal is only the scattering body, and light scattering from clusters is negligible because they are considered to be too small to be detected. Considering the experimental conditions of SLS, r, λ, ε, ε_0 and θ are constant amount the parameters in Eq. 1. Thus, Eq. 1 can be simply rewritten as

$$I_s/I_o = KV(t)^2N(t), \tag{2}$$

using time-dependent V and N and a constant K. The injection time is set to $t = 0$. In this model, $N(t)$ is also constant (N) through the crystal growing process, as mentioned above. The cluster numbers included into microcrystals per unit period are considered to be proportional to the number of remaining clusters. When the cluster number at time t is expressed as $N_c(t)$, this relation is

$$\mathrm{d}N_c(t)/\mathrm{d}t = -\alpha(T)N_c(t), \tag{3}$$

where $\alpha(T)$ is the crystal growth rate constant as a function of the temperature (T). Since the increment of the microcrystal volume should coincide with the summation of the combined cluster volume,

$$\mathrm{d}V(t)/\mathrm{d}t = -V_c(\mathrm{d}N_c(t)/\mathrm{d}t) \tag{4}$$

is obtained, where V_c is the cluster volume. When the cluster number at the initial stage is represented by $N_c(0)$, it can be expressed by using $N_c(t)$, N, V_c, and $V(t)$ as follows:

$$N_c(0) = N_c(t) + NV(t)/V_c. \tag{5}$$

Then, the relations described in Eqs. 3 and 5 are substituted into Eq. 4, and the following equation is derived:

$$\mathrm{d}V(t)/\mathrm{d}t = \alpha(T)N[V(\infty) - V(t)]. \tag{6}$$

Under the initial condition that $N_c(0)V_c$ should be equal to $NV(\infty)$, Eq. 6 can be solved to give

$$V(t) = V(\infty)[1 - \exp(-\alpha(T)Nt)], \tag{7}$$

using $V(0) = 0$. From Eqs. 2 and 7,

$$I_s/I_o = KV(\infty)^2[1 - \exp(-\alpha(T)Nt)]^2N \tag{8}$$

is obtained.

Equation 8 could reproduce the experimental results shown in Figs. 3 and 4. In the case of the experiment shown in Fig. 3, even though the amount of injection was varied, the final crystal size determined by DLS, which is closely related to $V(\infty)$, was found to be almost the same. Therefore, the final I_s/I_o values were mainly affected by N. Since the final I_s/I_o values were roughly proportional to the injection amount, N also seemed to be proportional to the injection amount if the concentration of the solution used was the same. In Fig. 4, the crystal growth-rate change, related to the magnitude of the tangential slope of the curves, clearly shows a temperature dependency. For the data at temperatures above 35 °C, the curves calculated using Eq. 8 are shown in Fig. 6, and are very similar to the experimental results shown in Fig. 4. One can determine the constant α_{app} corresponding to $\alpha(T)N$ in Eq. 8 by fitting the experimental data in Fig. 4. Arrhenius plots for microcrstal growth could be drawn, as presented in Fig. 7. By line-fitting to these plots, the apparent activation energy for perylene microcrystal growth in the reprecipitation method was determined to be 68 kJ mol^{-1}. From the view that the heat of fusion and sublimation from perylene crystals are, respectively, 32 and 126 kJ mol^{-1}, the crystallization from the cluster is supposed to progress via an isolated molecular state close to the gas phase. The obtained knowledge would be useful for preparing smaller and monodispersed organic microcrystals in the near future.

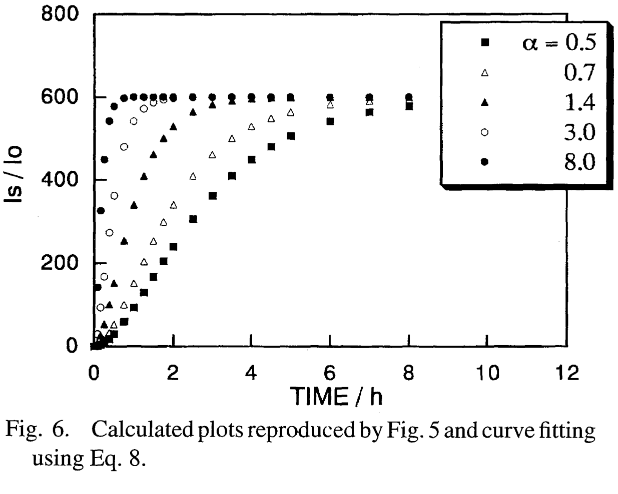

Fig. 6. Calculated plots reproduced by Fig. 5 and curve fitting using Eq. 8.

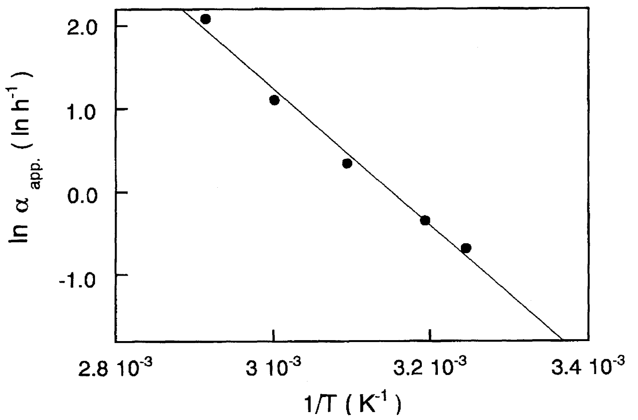

Fig. 7. Arrhenius plots for microcrystal growth of perylene in the reprecipitation method.

Concluding Remarks

In conclusion, the crystal growth of perylene microcrystals was investigated by performing measurements with light scattering and absorption spectroscopy. The microcrystallization process could be explained semi-quantitatively by the model proposed in this paper.

References

1) J. Depasse and A. Watilon, *J. Colloid Interface Sci.*, **33**, 430 (1970).

2) Y. Taketa, "Cho-biryushi (Ultrafine Particles)," ed by the Chemical Society of Japan, Gakkai Shuppan Center, Tokyo (1985); *Kagaku Sousetsu*, No. 48, p. 193 (in Japanese).

3) R. Kubo, *J. Phys. Soc. Jpn.*, **17**, 975 (1962).

4) E. Hanamura, *Phys. Rev. B*, **37**, 1273 (1988).

5) L. E. Brus, *J. Chem. Phys.*, **80**, 4403 (1984).

6) A. I. Ekimov, Al. L. Efros, and A. A. Onushchenko, *Solid State Commun.*, **56**, 921 (1985).

7) A. Nakamura, H. Yamada, and T. Tokizaki, *Phys. Rev. B*, **40**, 8585 (1989).

8) Y. Wang, *J. Opt. Soc. Am. B*, **8**, 981 (1991).

9) M. Fujitsuka, R. Nakahara, T. Iyoda, T. Shimidzu, and H. Tsuchiya, *J. Appl. Phys.*, **74**, 1283 (1993).

10) F F. So, S. R. Forrest, Y. Q. Shi, and W. H. Steier, *Appl. Phys. Lett.*, **56**, 674 (1990).

11) A. Matsui, *Mem. Konan Univ., Sci. Ser.*, **42**, 9 (1995), (in Japanese).

12) H. Toyotama, *Kinouzairyo*, **6**, 44 (1987), (in Japanese).

13) K. Yase, T. Inoue, M. Okada, T. Funada, and J. Hirano, *Hyomen Kagaku*, **8**, 434 (1989), (in Japanese).

14) H. Kasai, H. S. Nalwa, H. Oikawa, S. Okada, H. Matsuda, N. Minami, A. Kakuta, K. Ono, A. Mukoh, and H. Nakanishi, *Jpn.*

J. Appl. Phys., **31**, L1132 (1992).

15) H. Kasai, H. Kamatani, S. Okada, H. Oikawa, H. Matsuda, and H. Nakanishi, *Jpn. J. Appl. Phys.*, **35**, L221 (1996).

16) H. Kasai, Y. Yoshikawa, T. Seko, S. Okada, H. Oikawa, H. Matsuda, A. Watanabe, O. Ito, H. Toyotama, and H. Nakanishi, *Mol. Cryst. Liq. Cryst.*, **294**, 173 (1997).

17) R. Iida, H. Kamatani, H. Kasai, S. Okada, H. Oikawa, H. Matsuda, A. Kakuta, and H. Nakanishi, *Mol. Cryst. Liq. Cryst.*, **267**, 95 (1995).

18) H. Nakanishi and H. Kasai, "Polymers for Avanced Optical Applications," ed by A. Jenekhe and K. J. Wynne, ACS Press, Washington, DC, ACS Symposium Series, **672**, 183 (1997).

19) H. S. Nalwa, H. Kasai, S. Okada, H. Matsuda, H. Oikawa, H. Minami, A. Kakuta, K. Ono, A. Mukoh, and H. Nakanishi, *Polym. Adv. Technol.*, **6**, 69 (1995).

20) H. Kasai, H. Kanbara, R. Iida, S. Okada, H. Matsuda, H. Oikawa, and H. Nakanishi, *Jpn. J. Appl. Phys.*, **34**, L1208 (1995).

21) H. Kasai, R. Iida, H. Kanbara, S. Okada, H. Matsuda, H. Oikawa, T. Kaino, and H. Nakanishi, *Nonlinear Opt.*, **15**, 263 (1996).

22) H. Katagi, H. Kasai, S. Okada, H. Oikawa, K. Komatsu, H. Matsuda, Z. Liu, and H. Nakanishi, *Jpn. J. Appl. Phys.*, **35**, L1364 (1996).

23) H. Katagi, H. Kasai, S. Okada, H. Oikawa, H. Matsuda, and H. Nakanishi, *J. Macromol. Sci. -Pure Appl. Chem.*, **A34**, 2013 (1997).

24) J. Tanaka, *Bull. Chem. Soc. Jan.*, **36**, 1237 (1963).